Egypt. J. Geo. **Vol 66,** pp: 25-40 (2022)

Egyptian Journal of Geology
https://egjg.journals.ekb.eg

Reservoir Characterization of the Upper Cretaceous Abu Roash and Bahariya Reservoirs, Main Abu El-Gharadig Oil Field, North Western Desert, Egypt

Nader H. El-Gendy[1], Mohamed A. Noweir[1], Mohamed S. El-Sadek[2], Ahmed S. Ali[1]
[1]Geology Department, Faculty of Science, Tanta University, Tanta 31527, Egypt
[2]Khalda Petroleum Company, Cairo, Egypt

THE study area is located in Abu El-Gharadig basin, between 29° 40' and 29° 45' N latitudes and 28° 25' and 28° 32' E longitudes. The study aims to evaluate four formations that are located in the middle part of Abu El-Gharadig Basin, North Western Desert, Egypt. This is carried out by conducting petrophysical analysis, to investigate the late Cretaceous hydrocarbon-bearing reservoirs of the Abu Roash "D" and "E" Members, and the Bahariya Formations. To achieve the aim, **Interactive Petrophysics software (IP) version 3.5** helped in well-logging evaluation providing the density-neutron and the M-N cross_plot, to characterize the porosity and lithology of the reservoirs and the effect of shale and secondary porosity on the potentials of these reservoirs. In addition, the software presents analogs indicating the vertical distribution of petrophysical parameters for the studied well and to show the distribution of shale volume, porosity, water saturation and hydrocarbon saturation and identify the oil-bearing zones. Analysis of the petrophysical parameters report that, the Abu Roash "D" reservoir is mostly limestone with sandstone and shale lithology, while the Abu Roash "E" reservoir is primarily sandstone, with shale, limestone and dolomite lithology. The reservoirs in the Upper and Lower Bahariya are mostly sandstones, with argillaceous and calcareous types of cement. The shale volumes in the Abu Roash (D and E) Members and Upper and Lower Bahariya Formation are 0.9 – 3.8 %, 8.2 – 13.7, 7.2 – 15.2, and 9 – 15.5 %, respectively, and the effective porosities are 6.7 – 14.7 %, 13.9 – 18.1 %, 13.1 – 15.5 % and 11.4 – 15.5 %, expressing a good reservoir quality of the zones. Petrophysical data from the Abu Roash and Bahariya reservoirs are shown on analogs, to identify the most effective thicknesses with good hydrocarbon potential.

Keywords: Formation Evaluation, well logs, Abu Roash and Bahariya Reservoirs, Abu El-Gharadig Basin.

Introduction

Oil exploration and production in the Western Desert have a long history. The northern Western Desert has huge oil and gas potentials, although the fact that, just a few discoveries have been made to date. The Abu El-Gharadig basin is located in the Western Desert's northern region. The Main Abu El-Gharadig oil field is located in the Abu El- Gharadig basin's central part. The Upper Cretaceous reservoirs are the primary producing horizons at Abu El- Gharadig oil field.

The study located is located in the Abu El-Gharadig basin, between 29° 40' and 29° 45' N latitudes and 28° 25' and 28° 32' E longitudes (**Fig. 1**). The followings are the work major steps: 1) Determination of the reservoir porosity and lithology, using various crossplots, 2) Identification of the various reservoir parameters'

*Corresponding author: ahmed.ali@science.tanta.edu.eg
Recived: 29/05/2022; Accepted: 23/06/2022;
DOI: 10.21608/EGJG.2022.139760.1020

describing the pay-zones, using the data acquired from the well logs to highlight attractive places for further development and investigate the production potential of the Abu Roash (D & E) and Bahariya reservoirs (Upper & Lower) in the Main Abu El- Gharadig oil field, north Western Desert, Egypt.

Bakr (1990) described the Jurassic and/or Lower Cretaceous structural setting of the sedimentary basins in the northern Western Desert, close to their large basin-surrounding faults. The NE to ENE folding trend' related to the reverse faulting are the main prominent geological structures in the northern Western Desert. The majority of those faults occurred in the Late Cretaceous to the Early Tertiary time, where the E-W faults show mark of strike-slip movements along the previously pre-existing faults **(Sultan and Abd El-Halim, 1988).**

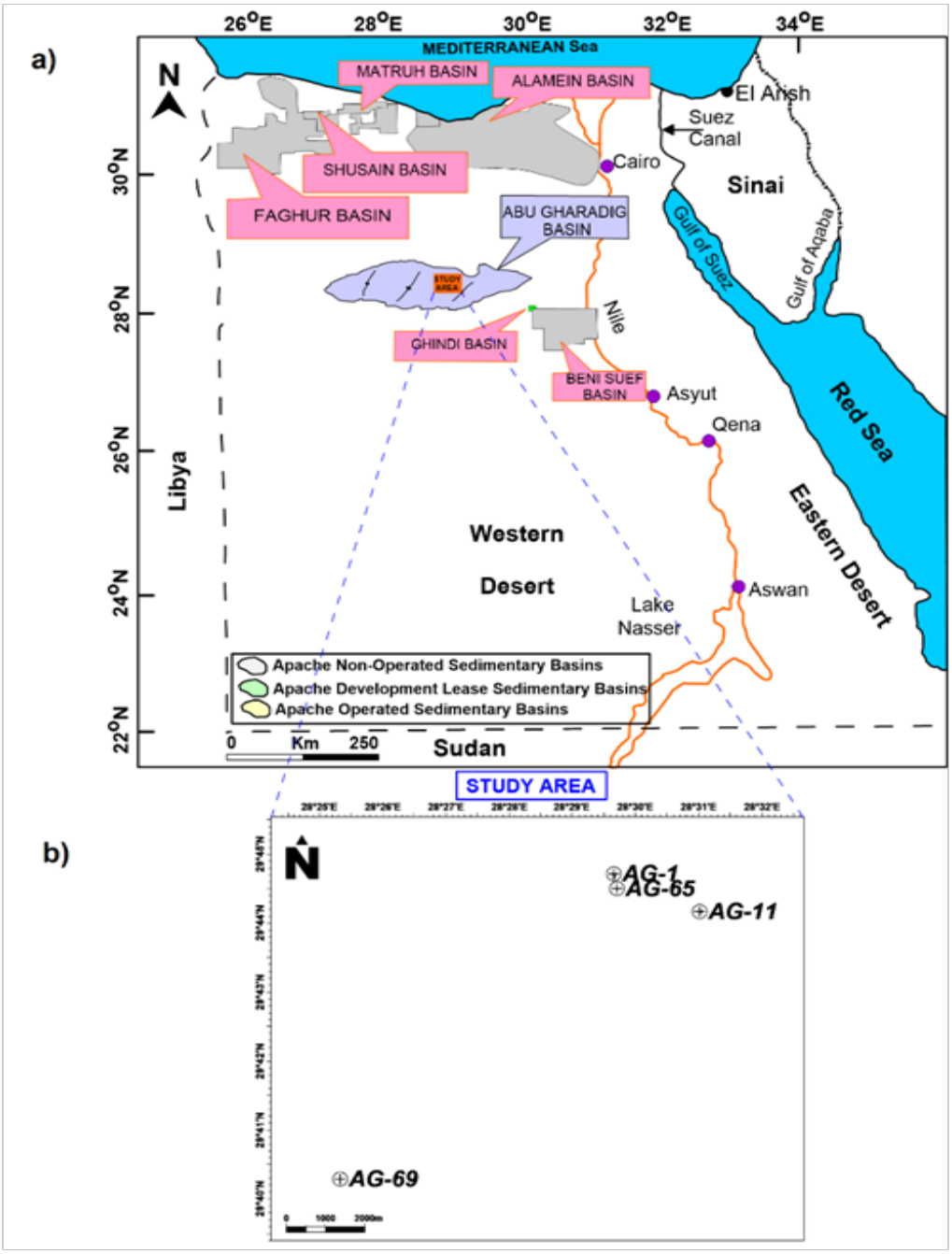

Fig. 1. Location map shows the studied area (a) and the four studied well of the evaluated area (b).

The northern Western Desert's generalized stratigraphic column **(Fig. 2)** contains the majority of the sedimentary succession, begging from the Cambrian till reaching the Miocene **(Schlumberger 1995).** The whole sedimentary succession rested unconformably on the Pre-Cambrian basement complex. The Formation of Abu Roash is distinguished into seven lithostratigraphic Mbs (A to G), each of which covers the Late Cenomanian to Coniacian time intervals and reaches thicknesses of up to 1000 m in the Abu Gharadig depocenter, containing a significant portion of the oil discovery reserves **(Schlumberger, 1984)**. Fine clastics comprise members' A, C, E and G, while the clean carbonates form members' B, D and F. The Abu Roash Formation's lower contact is located at the base of the Abu Roash "G" Member, which is rested unconformably on the Bahariya Formation. When the Khoman Formation is missed, the upper contact of the Abu Roash Formation is the lower surface of the Khoman Formation. The upper contact of this unit has been proven to be an unconformity surface, throughout many areas of the Western Desert **(EGPC, 1992).**

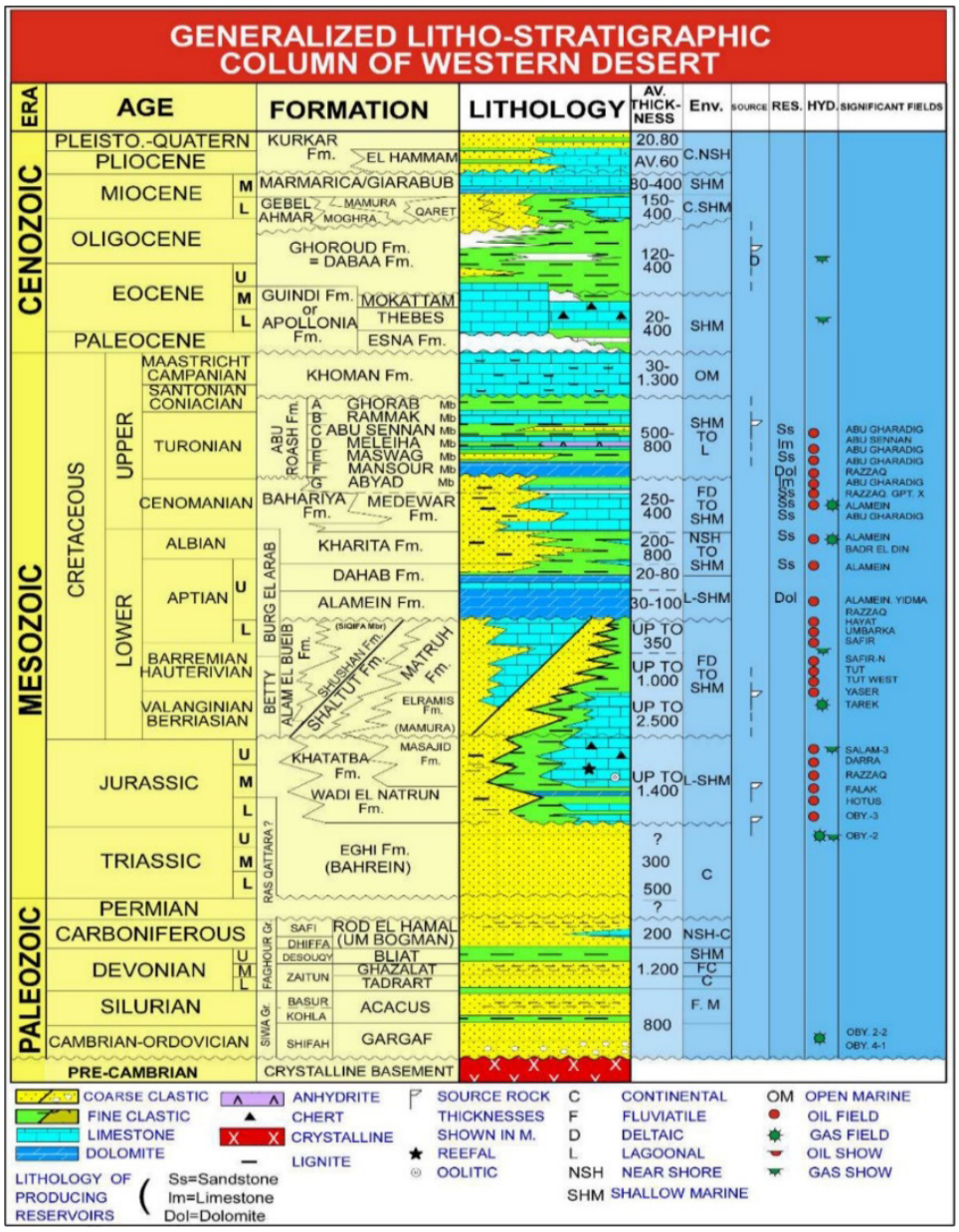

Fig. 2. Generalized litho-stratigraphic column for North Western Desert, Egypt (Schlumberger, 1995).

The age of the Bahariya Formation is Early Cenomanian. It's made up of sandstone with fine to very fine grains and shale. Glauconite and pyrite are common, as thin limestone strata appear in random patterns and are difficult to connect from one well to another **(EGPC, 1992)**. The major gas and/or condensate pay, in the Abu El Gharadig basin, is the Bahariya sandstones. It marks a gradational phase of finning upwards to the Turonian-Coniacian Abu Roash Formation's marine carbonates and shales.

Methodology

AG-1X, AG-11, AG-65 and AG-69 are the wells, that were investigated. The available well logs used in this study are density, sonic, resistivity, gamma-ray, caliper and neutron logs.

Determination of lithology and porosity from crossplots

The lithologies of the Abu Roash (D & E) and (Upper & Lower) Bahariya were interpreted, using all the logs, that were registered systematically, and the lithology was determined from logs, using several cross plots (Neutron / Density and M / N cross plots).

Petrophysical evaluation

Evaluation of well logs is analyzed using **Interactive Petrophysics software (IP), version 3.5**. The distribution of the total thickness, shale volume, effective porosity, total porosity, net-pay thickness, net/gross thickness, hydrocarbon saturation, water saturation, residual hydrocarbon saturation and movable hydrocarbon saturation are shown, using petrophysical parameters extracted from well log data for the Abu Roash (D & E) and (Upper & Lower) Bahariya reservoirs.

Results and Interpretation

Determination of lithology and porosity from density-neutron crossplots

Density-neutron crossplots are often used to detect lithology and precisely estimate the matrix (non-shaly) porosity of carbonate rocks, using neutron and density logs. The bulk density and neutron porosity data are plotted together in this situation. Lines (quartz, limestone, dolomite, …etc.) corresponding to certain water-saturated and pure lithologies can be graduated in porosity units, or a single zero-porosity point can be established. The point drawn from the log measurements falls between the lithology lines, when the matrix lithology is a binary mixture, such as Quartz-Lime or Lime-Dolomite. The light HC's (gas) impact can be seen on the crossplot, at which the displayed data tend to move north westerly from the sandstone line, because this impact enhances density log porosity identifications, while reducing neutron porosity. In addition, the shale impact may be seen on the crossplot, in which the shale influence seems to be in the lower right quadrant. **(Poupon and Leveaux, 1971).**

From the density-neutron crossplot of Abu Roash "D" reservoir (**Fig. 3**), it is seen that, nearly all the drawn points are dispersed on the limestone line and a few points between the sandstone and limestone lines, and limestone and dolomite lines with porosity values are in between 1 to 20 %. This indicates that, the reservoir is commonly limestone with some sandstone and dolomite lithologies.

From the density-neutron crossplot of the Abu Roash "E" reservoir (**Fig. 4**), it is noticed that the displayed points are dispersed close to the sandstone line and the other points between the sandstone, limestone and dolomite lines, with porosity values are in between 1 to 30 %. This indicates that, the reservoir is mainly sandstone, with some limestone and dolomite lithologies. Some points were drawn upward, because of the gas effect and few points are seen in the lower right quadrant of the chart, due to the shale effect.

From the density-neutron crossplot of the Upper Bahariya reservoir (**Fig. 5**), we can see that most of the drawn points are dispersed close to the sandstone line and the other points between the sandstone, limestone and dolomite lines, with porosity values are in between 1 to 35%. This indicates that, the reservoir is mainly sandstone, with carbonate lithology. Some points are displayed upward, because of the gas impact.

From the density-neutron crossplot of the Lower Bahariya reservoir (**Fig. 6**), it is clear that most of the displayed points are dispersed close to the sandstone line and above it, and the other points between the sandstone, limestone and dolomite lines, with porosity values are in between 6 to 38%. This indicates that, the reservoir is commonly sandstone, with limestone and dolomite lithologies. The number of points is scattered upward, due to the gas effect.

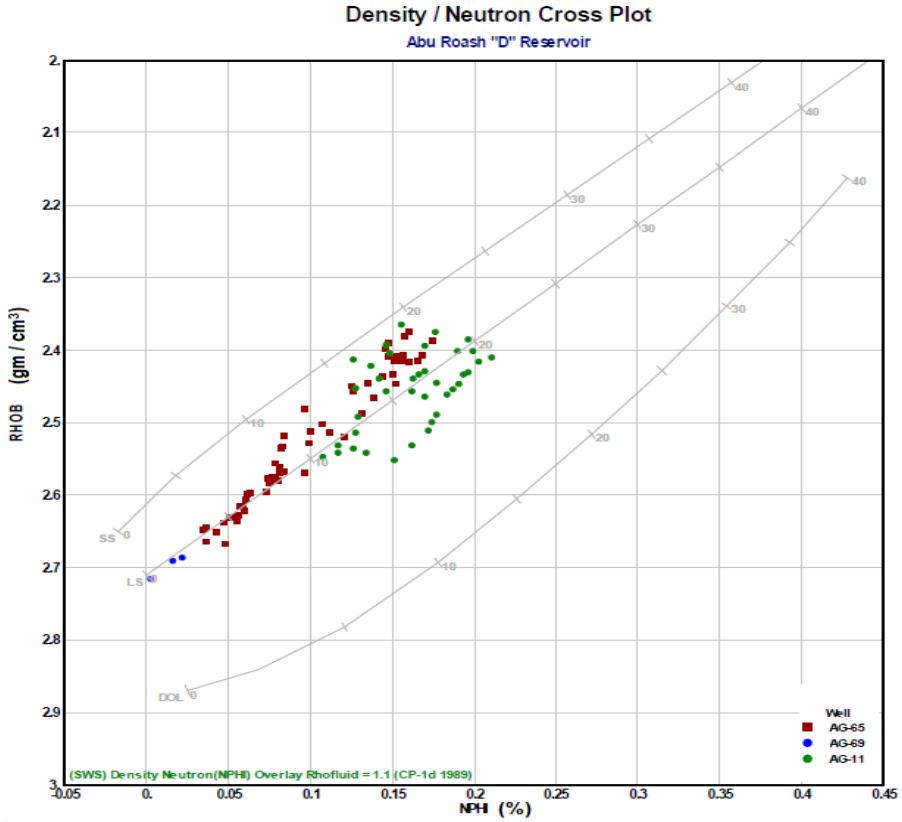

Fig. 3. Density-neutron crossplot of the Abu Roash "D reservoir.

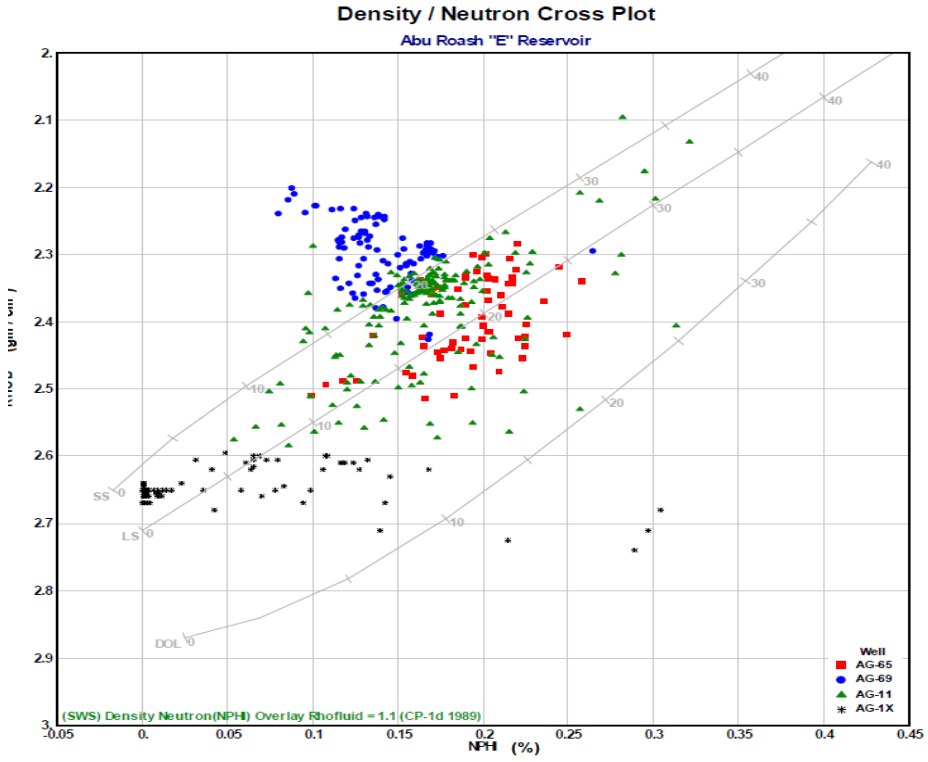

Fig. 4. Density-neutron crossplot of the Abu Roash "E reservoir.

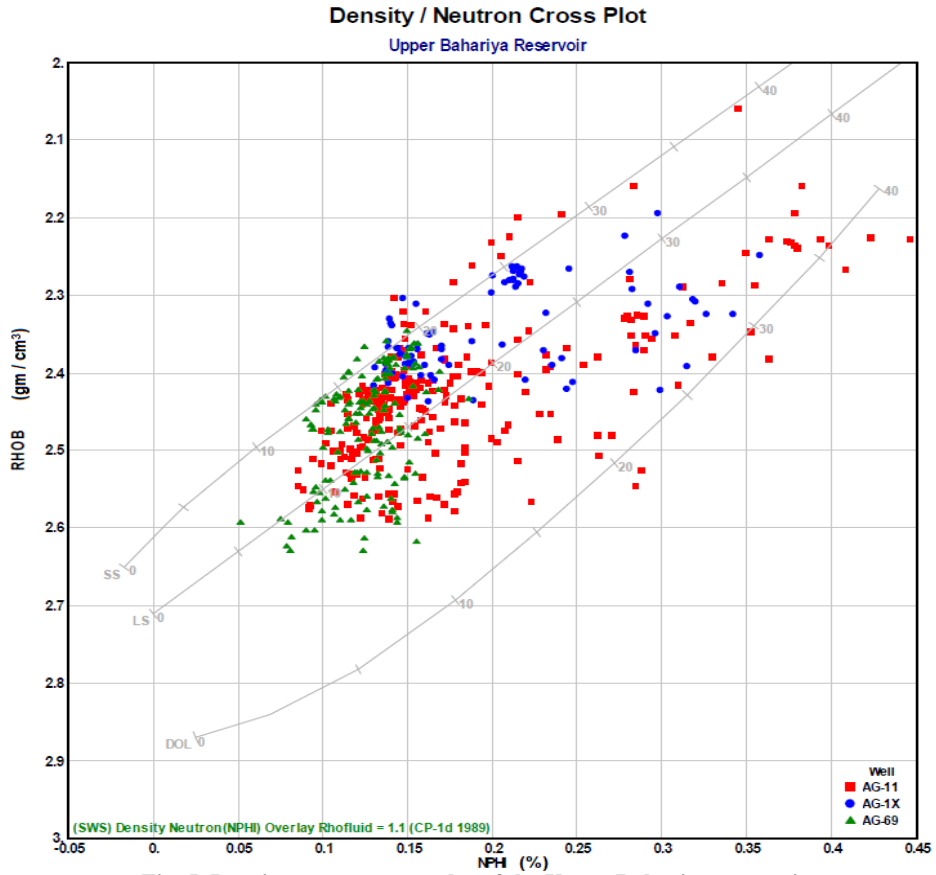

Fig. 5. Density-neutron crossplot of the Upper Bahariya reservoir.

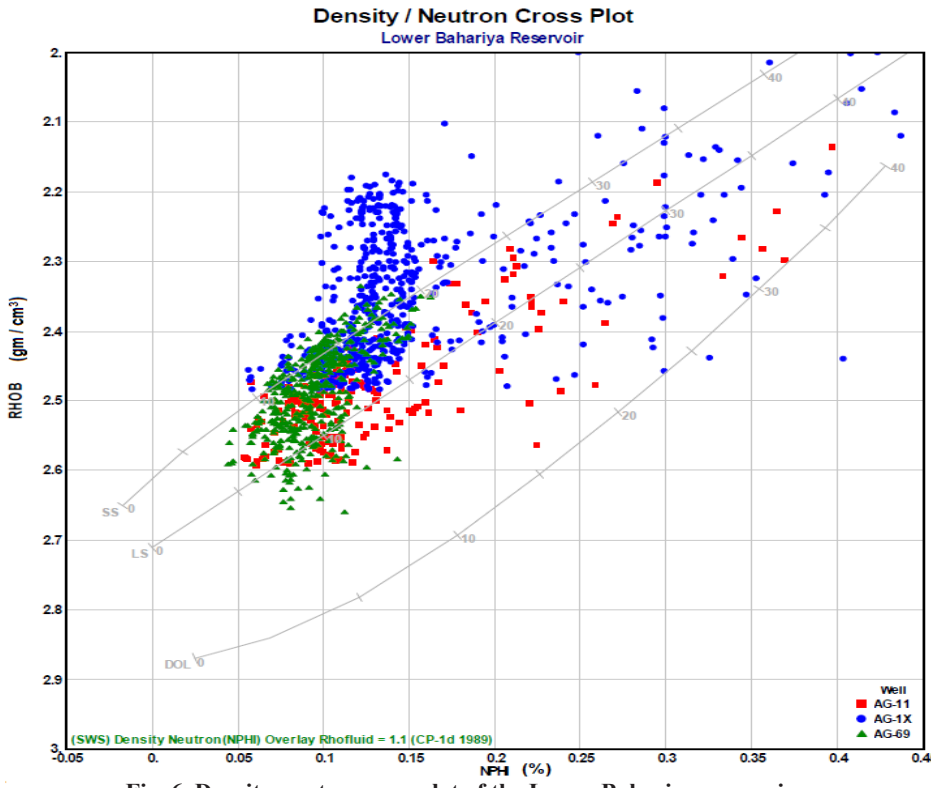

Fig. 6. Density-neutron crossplot of the Lower Bahariya reservoir.

Lithology identification using M-N crossplots

The M–N plot is useful for lithology identification in more complex mineral compositions. The lithology-dependent values M and N are plotted, using the data combined from all the three porosity logs **(Schlumberger, 1989)**. A sonic log, as well as neutron and density logs, are required for the M–N plot. The sonic log is a porosity log, that detects interval the transit time. The reciprocal of the velocity of a compressional sound wave through one foot of formation is the interval transit time (Δt). To calculate the lithology-dependent variables, M and N, sonic, density and neutron logs are required. M and N values are unconstrained of the matrix porosity (sucrosic and intergranular) **(Asquith and Gibson, 1982)**. When these two variables are plotted together, the lithology becomes more obvious. The following equations are used, to calculate the M and N values. **(Schlumberger, 1972):**

$$M = ((\Delta tf - \Delta t))/((\rho b - \rho bf) \times 0.01) \quad (1)$$

$$N = ((\varphi Nf - \varphi N))/((\rho b - \rho bf)) \quad (2)$$

Where;

Δtf = is the interval transit time of the mud fluid,

Δt = is the sonic log value,

Pb = is the density log value,

ρbf = is the density of mud fluid,

φNf = is the neutron of mud fluid,

φN = is the neutron log value.

Shaliness, secondary porosity and gas-filled porosity lead the M-N points to lie out of the triangle region indicated, by the primary mineral elements, causing them to shift with respect to their real lithology. Secondary porosity is indicated by the upward displacement of the plotted points, whereas the influence of gas might cause the points to shift upward on the right. Because shales vary in their features, there are no specific shale points on the M-N plot. The shale effect is usually found under the line, which connects the anhydrite and silica points **(Bigelow, 1995)**.

Figure (**7**) indicates the mineralogic constitution of Abu Roash "D" reservoir of the study area. Most samples were dispersed to fill the calcite part and the parts between calcite and quartz, although they appear to be near the calcite part than the quartz one. This may reflect the occurrence of a limestone reservoir. Some points were scattered upwards, due to the secondary porosity influence.

Figure (**8**) reveals the mineralogic composition of the Abu Roash "E" reservoir in the study area. Most samples were dispersed to fill the quartz part and the parts between quartz and calcite, although they appear to be near the quartz part than the calcite one. This may reflect the occurrence of a sandstone reservoir, with some calcareous cement. Many points are dispersed downwards, because of the shale impact and others are dispersed upward, as a result of the secondary porosity influence.

Figure (**9**) indicates the mineralogic constitution of the Upper Bahariya reservoir in the study area. Most samples are dispersed to fill the quartz part and the parts between quartz, calcite and dolomite, but they are very close to the quartz part than the calcite and dolomite. This may reflect the occurrence of sandstone reservoir, accompanied by some calcareous cement. Some points are dispersed downward, because of the shale impact. The influence of gas could be seen in shifting the dispersed points in the upright corner of the diagram. The rest of the points are shifted upward, as a result of the secondary porosity influence.

Figure (**10**) reveals the mineralogic constitution of the Lower Bahariya reservoir in the study area. Most samples are dispersed to fill the quartz part and the parts between quartz, calcite and dolomite, but they are very close to the quartz part than the calcite and dolomite. This may reflect the occurrence of sandstone reservoir, accompanied by some carbonate lithology. Number of points are dispersed downward, because of the shale impact. The influence of gas could be seen in shifting the drawn points in the upright corner of the diagram.

Vertical distribution of petrophysical parameters

The petrophysical parameters derived from well-log analysis show vertical variation in general. To accomplish the study of hydrocarbon potentials in the concerning area under investigation, the vertical variance of petrophysical features might be analyzed, using some gradients **(Tearpock & Bischke, 2003)**. Table (**1**) displays the reservoir characteristics determined from the average of various log parameters.

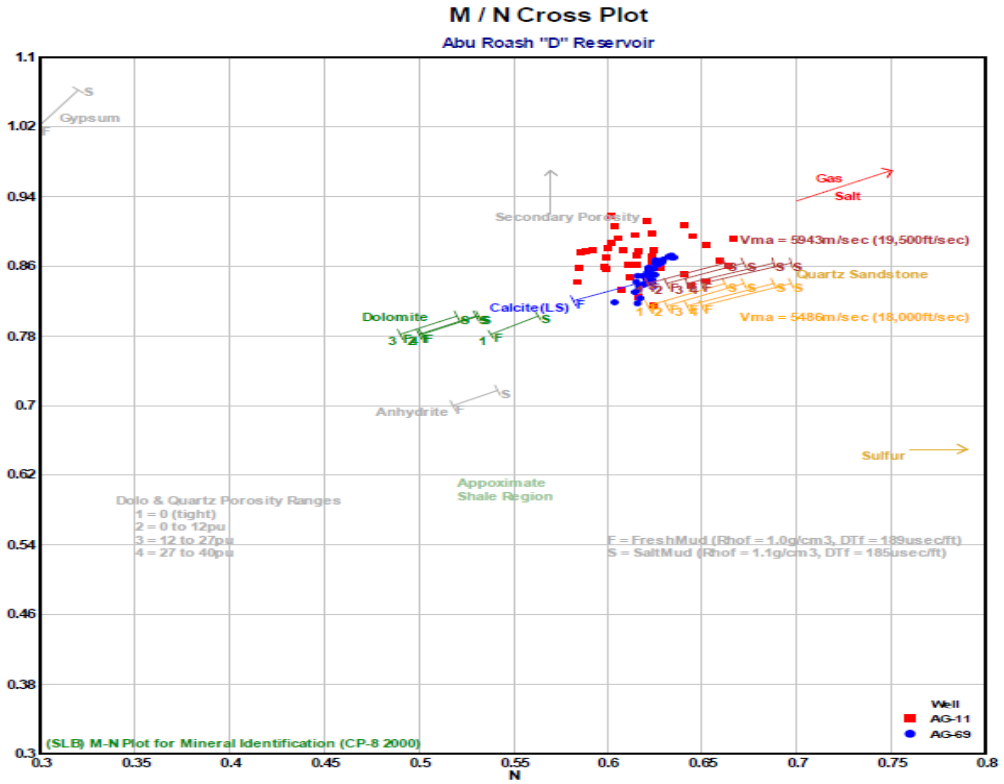

Fig .7. The M – N crossplot of Abu Roash "D" reservoir.

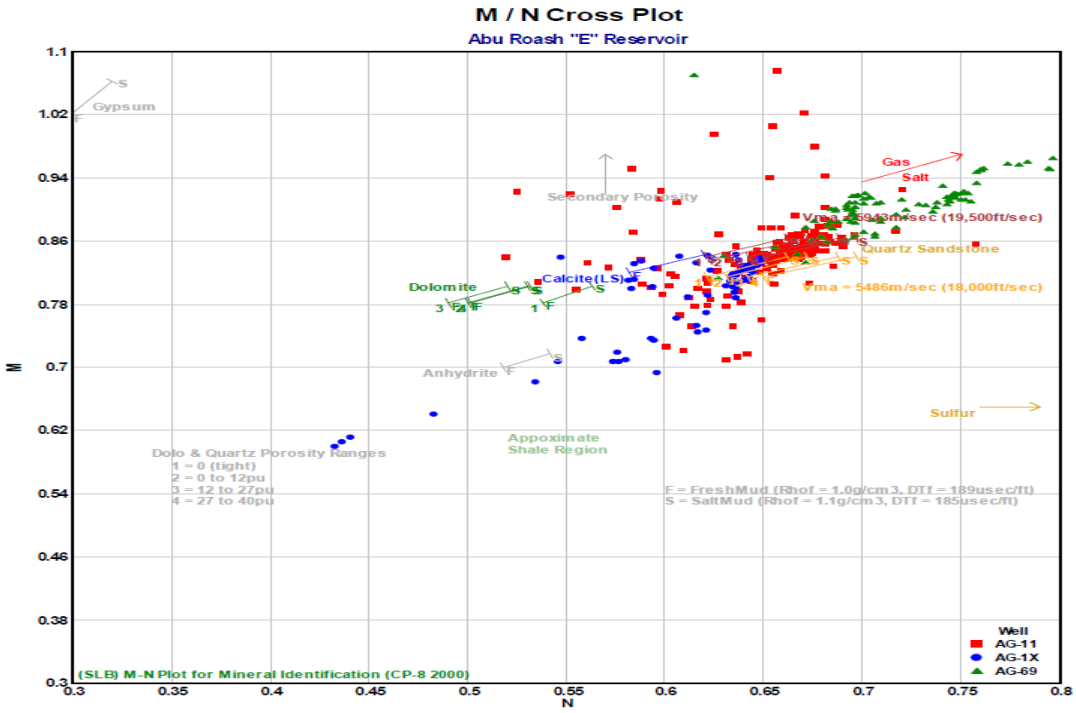

Fig. 8. The M – N crossplot of Abu Roash "E" reservoir.

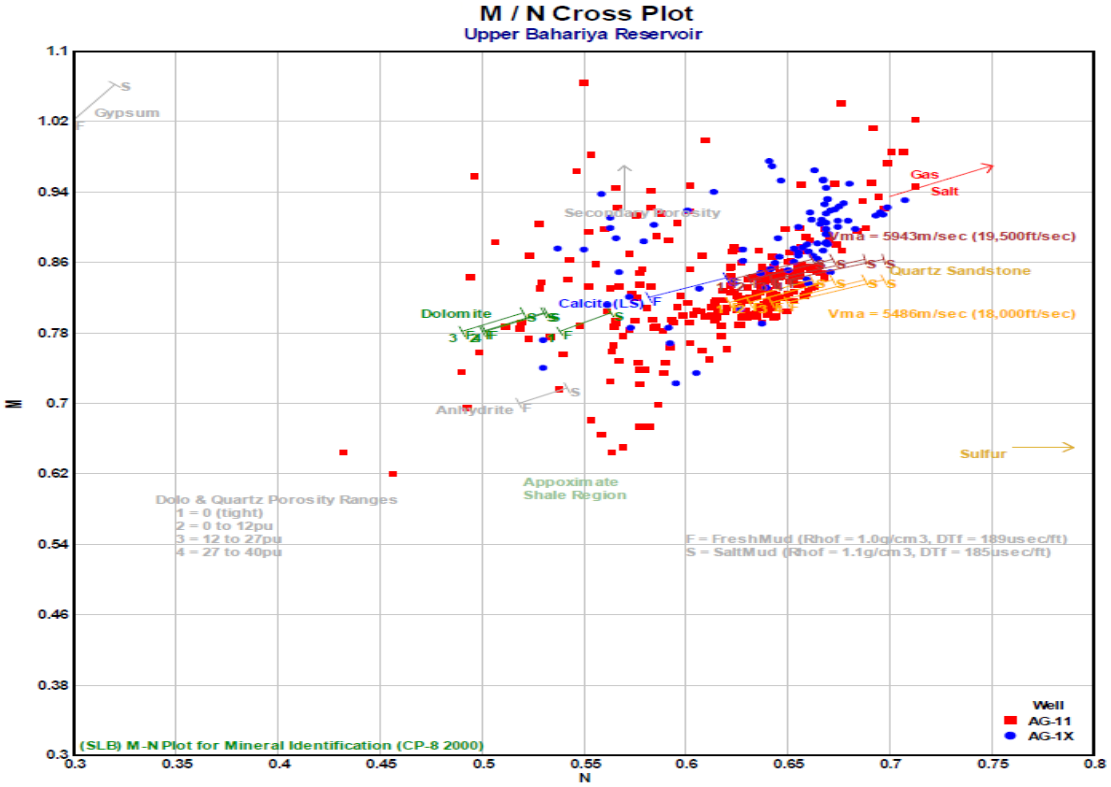

Fig. 9. The M – N crossplot of Upper Bahariya reservoir.

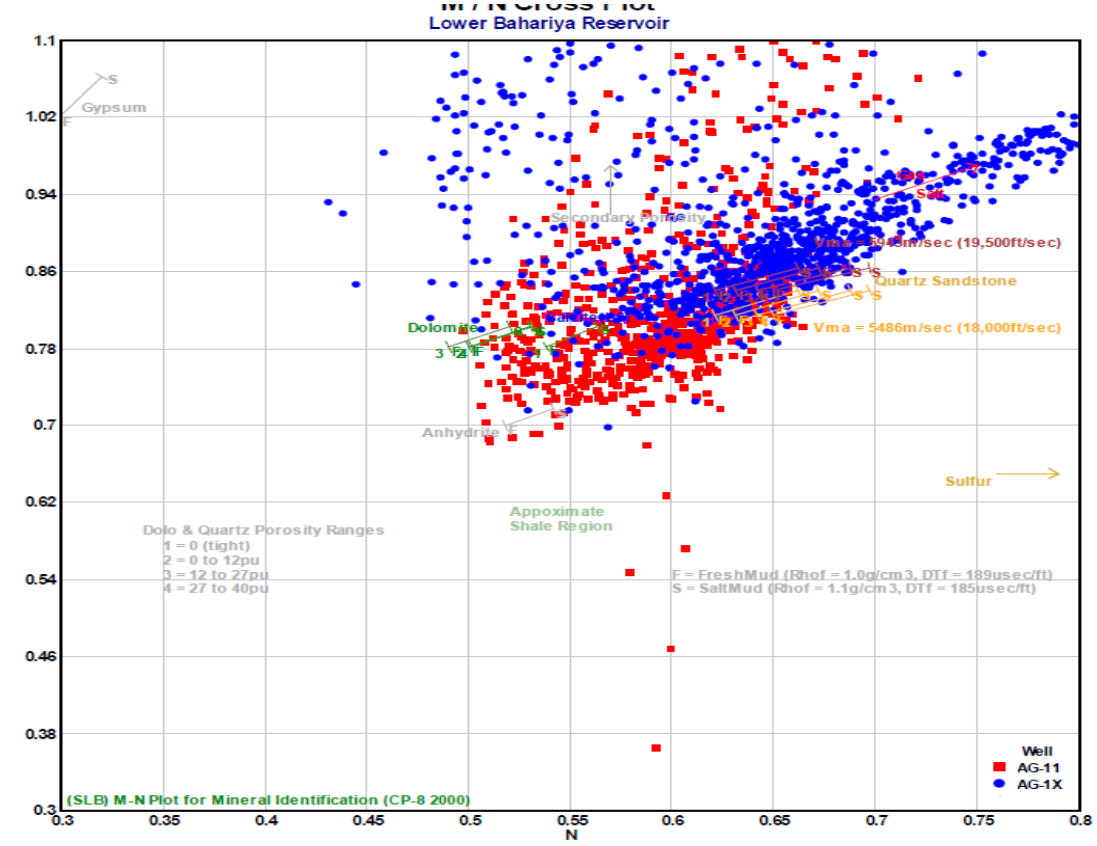

Fig. 10. The M – N crossplot of Lower Bahariya reservoir.

TABLE 1. Parameters of well Log results of the Abu El-Gharadig oil field, Western Desert, Egypt.

WELL	Reservoir	Total Thickness (ft)	Total Porosity (%)	Effective Porosity (%)	Shale Volume (Vsh, %)	Net pay (ft)	Net / Gross (N/G, %)	Water Saturation (Sw, %)	Hydrocarbon Saturation (Sh, %)	Residual Hydrocarbon Saturation (Shr, %)	Movable Hydrocarbon Saturation (Shm, %)
AG - 1X	A / R - D	Missed									
AG - 11		370.5	16.2	14.7	3.8	18	100.0	25.1	74.9	65.3	9.6
AG - 65		403.5	15.3	14.7	3	11.5	100.0	13.5	86.5	86.3	0.2
AG - 69		203	6.7	6.7	0.9	3.5	41.2	50	50	23.6	26.4
AG - 1X	A / R - E	459	16.5	13.9	13.7	0	0.0	93.4	6.6	6.1	0.5
AG - 11		467.5	19.4	15.7	8.2	57.5	97.5	24.9	75.1	65.5	9.6
AG - 65		351	20.1	18.1	11.3	14	49.1	40.2	59.8	59.7	0.1
AG - 69		460.5	19.4	16.8	10.9	53	100.0	25.9	74.1	24.5	49.6
AG - 1X	U. BAH.	496.5	17.8	15.5	15.2	47.5	97.9	27.1	72.9	60.9	12
AG - 11		312.5	16.4	13.1	8.2	54	100.0	26.9	73.1	60.2	12.9
AG - 65		Missed									
AG - 69		456	14.5	13.4	7.2	44.5	84.0	38.4	61.6	25.9	35.7
AG - 1X	L. BAH.	595	18	15.5	15.5	213.4	98.4	17.9	82.1	63.7	18.4
AG - 11		452	14	12.8	9	34.5	86.3	29	71	64	7
AG - 65		Missed									
AG - 69		448	13	11.4	13.4	0	0.0	94.5	5.5	2.8	2.7

The vertical distribution of petrophysical parameters was achieved by creating analogs (**Figs. 11 to 16**) for each well in the study area, to show the distribution of porosity, shale volume, water saturation and the hydrocarbon saturation. The analogs show the rock components and their fluid contents as a function of well depth. Clay minerals, quartz, dolomite minerals and calcite are rock constituents, whereas water and hydrocarbon are fluid constituents. The following is a brief description of the reservoir lithology and fluid contents in the investigated wells.

Abu Roash "D" reservoir

a) Abu Roash "D" reservoir analog in AG-11 well

The analog of Abu Roash "D" reservoir in AG-11 well shows that, the rock unit is composed of limestone, as main lithologic constituent, accompanied by thin streaks of sandstone and dolomite. The hydrocarbon saturation reveals an increase in the middle part of the reservoir **(Fig. 11)**.

b) Abu Roash "D" reservoir analog in AG-65 well

The analog of Abu Roash "D" reservoir in AG-65 well exhibits that, the rock unit is composed of limestone, as the main lithologic constituent, accompanied by layers of sandstone and siltstone. The hydrocarbon saturation reflects an increase in the lower middle part of the reservoir **(Fig. 12)**.

c) Abu Roash "D" reservoir analog in AG-69 well

The analog of Abu Roash "D" reservoir in AG-69 well represents that, the rock unit is composed of limestone, as a major lithologic constituent. The hydrocarbon saturation reveals an increase in the middle part of the reservoir **(Fig. 13)**.

Abu Roash "E" reservoir

a) Abu Roash "E" reservoir analog in AG-1X well

The analog of Abu Roash "E" reservoir in AG-1X well shows that, the rock unit is composed of sandstone, as a major lithologic constituent, with layers of siltstone, limestone, and dolomite. The water saturation reflects an increase in the top part of the reservoir **(Fig. 14)**.

b) Abu Roash "E" reservoir analog in AG-11 well

The analog of Abu Roash "E" reservoir in AG-11 well reveals that, the rock unit is composed of sandstone, as a major lithologic constituent, with layers of siltstone and dolomite. The hydrocarbon saturation reflects an increase at the top and central parts of the reservoir **(Fig. 11)**.

c) Abu Roash "E" reservoir analog in AG-65 well

The analog of Abu Roash "E" reservoir in AG-65 well represents that, the rock unit is composed of sandstone, as a major lithologic constituent, with layers of siltstone, limestone and dolomite. The hydrocarbon saturation reveals an increase at the top middle part of the reservoir **(Fig. 12)**.

d) Abu Roash "E" reservoir analog in AG-69 well

The analog of Abu Roash "E" reservoir in AG-69 well exhibits that, the rock unit is composed of sandstone, as a major lithologic constituent, with layers of siltstone and limestone. The hydrocarbon saturation shows an increase in the top middle part of the reservoir **(Fig. 13)**.

Upper Bahariya reservoir

a) Upper Bahariya reservoir analog in AG-1X well

The analog of the Upper Bahariya reservoir in AG-1X well reveals that, the rock unit is composed of sandstone, as a major lithologic constituent, with layers of siltstone and dolomite. The hydrocarbon saturation reflects an increase in the lower central and lower part of the reservoir **(Fig. 14)**.

b) Upper Bahariya reservoir analog in AG-11 well

The analog of the Upper Bahariya reservoir in AG-11 well represents that, the rock unit is composed of sandstone, as a major lithologic constituent, with layers of siltstone and dolomite. The hydrocarbon saturation reveals an increase in the middle part of the reservoir **(Fig. 15)**.

c) Upper Bahariya reservoir analog in AG-69 well

The analog of the Upper Bahariya reservoir in AG-69 well exhibits that, the rock unit is composed of sandstone, as a major lithologic constituent, with layers of siltstone, limestone and dolomite. The hydrocarbon saturation shows an increase in all the reservoir intervals **(Fig. 16)**.

Lower Bahariya reservoir

a) Lower Bahariya reservoir analog in AG-1X well

The analog of the Lower Bahariya reservoir in AG-1X well reveals that, the rock unit is composed of sandstone, as a major lithologic constituent, with layers of siltstone. The hydrocarbon saturation reflects an increase in all the reservoir intervals **(Fig. 15)**.

b) Lower Bahariya reservoir analog in AG-11 well

The analog of the Lower Bahariya reservoir in AG-11 well represents that, the rock unit is composed of sandstone, as a major lithologic constituent, with layers of siltstone, limestone and dolomite. The hydrocarbon saturation illustrates an increase in the central and top parts of the reservoir **(Fig. 15)**.

c) Lower Bahariya reservoir analog in AG-69 well

The analog of the Lower Bahariya reservoir in AG-69 well exhibits that, the rock unit is composed of sandstone, as a major lithologic constituent, with layers of siltstone and limestone. The water saturation shows an increase in all the reservoir intervals **(Fig. 16)**.

Conclusions

The presence of good quality reservoirs in the Abu Roash (D & E) and (Upper & Lower) Bahariya rock units are revealed by a detailed examination of the petrophysical characteristics from four wells located throughout the Abu El-Gharadig oil field.

The Abu Roash D Member's Density - Neutron and M-N cross-plots show primarily limestone, with some sandstone and dolomite lithologies, whereas the Abu Roash E Member's major lithology is sandstone, with some calcareous cement in all of the study area's wells. The lithology is mostly sandstone, with some carbonate lithology, according to the cross-plots of the Upper and Lower Bahariya layers. Furthermore, the effect of gas emerges in the diagrams, by shifting some points upward. Moreover, the shale effect is visible in the figures, by adjusting the distributed points in the upright corner of the diagrams.

The Abu Roash E Member's available well log data indicate good reservoir quality for oil production, with net-pay thicknesses of 57.5 ft and 53 ft in the AG-11 and AG-69 wells, respectively. Also, the net-pay is good for Upper Bahariya Member and reaches 47.5 ft, 54 ft and 44.5 ft in AG-1X, AG-11 and AG-69 wells, respectively. Furthermore, the Lower Bahariya Member appears to have good reservoir quality and the net-pay thickness reaches 213.4 ft and 34.5 ft in AG-1X and AG-11, respectively.

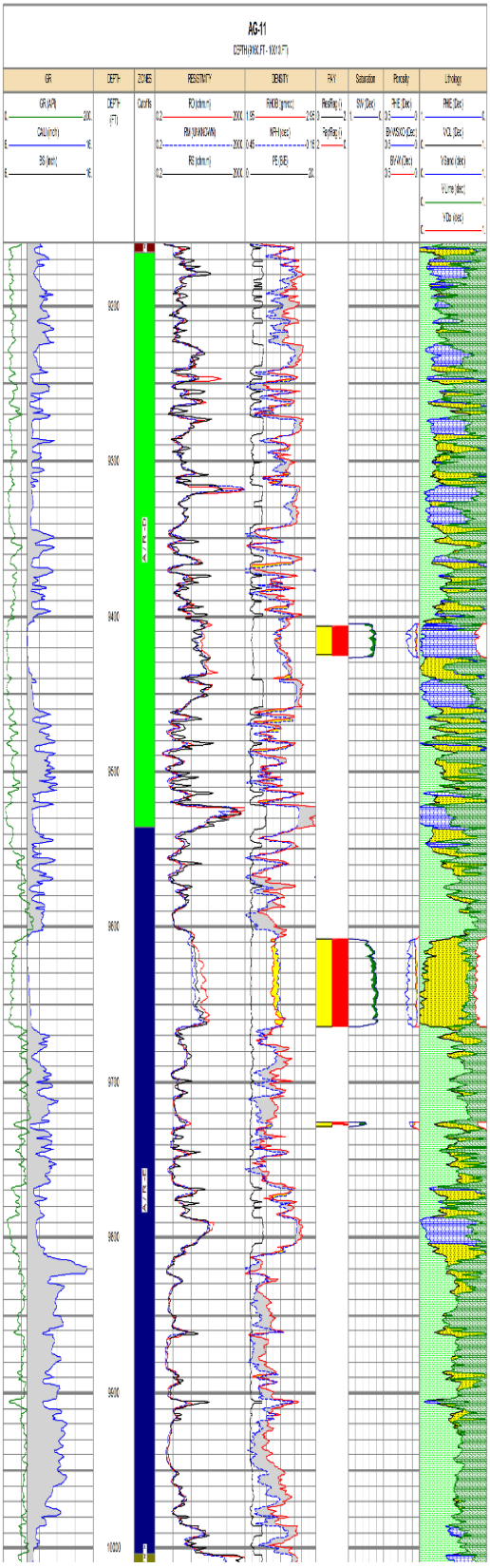

Fig. 11. Analog of Abu Roash "D" and "E" reservoirs in AG-11 well.

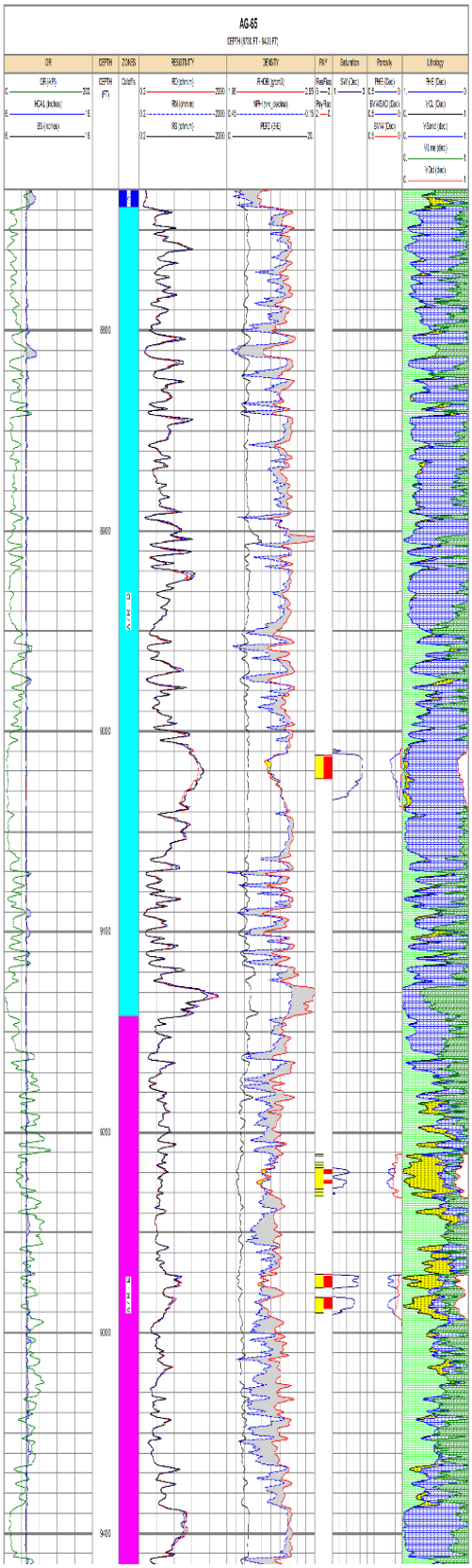

Fig. 12. Analog of Abu Roash "D" and "E" reservoirs in AG-65 well.

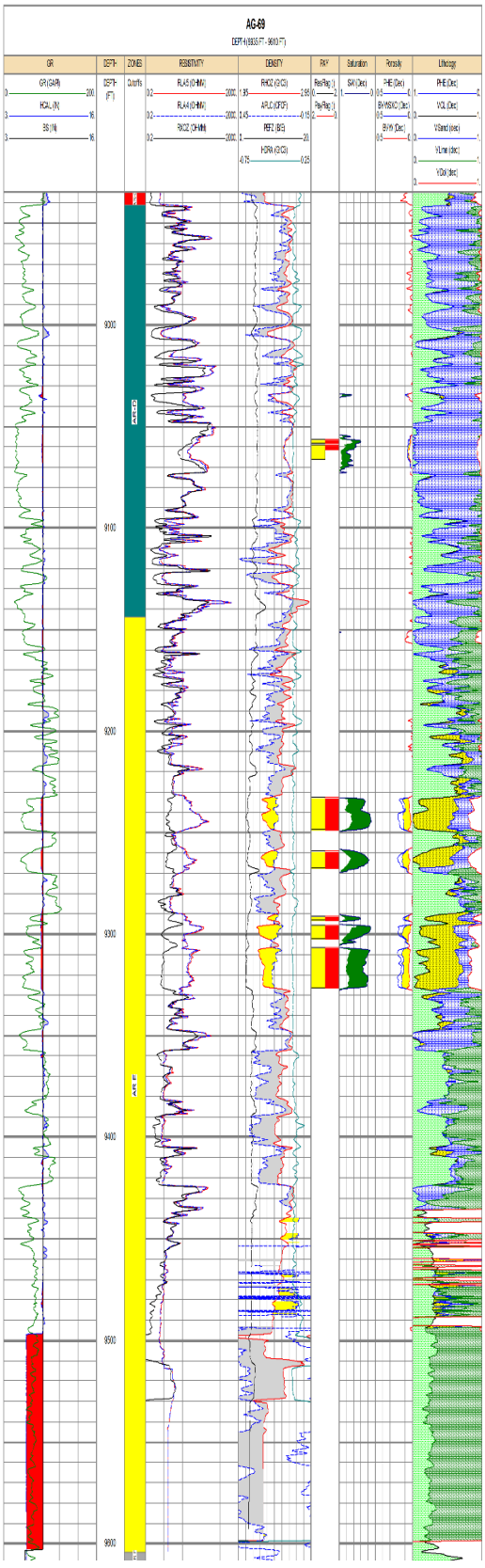

Fig. 13. Analog of Abu Roash "D" and "E" reservoirs in AG-69 well.

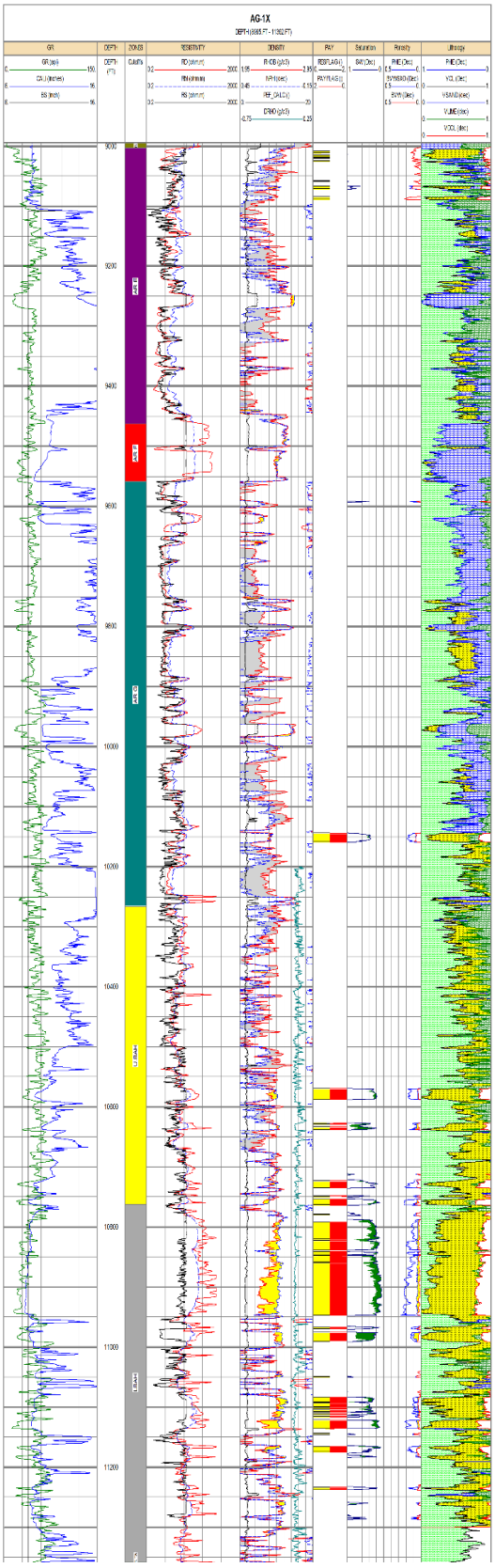

Fig. 14. Analog of Abu Roash "E" and Bahariya reservoirs in AG-1X well.

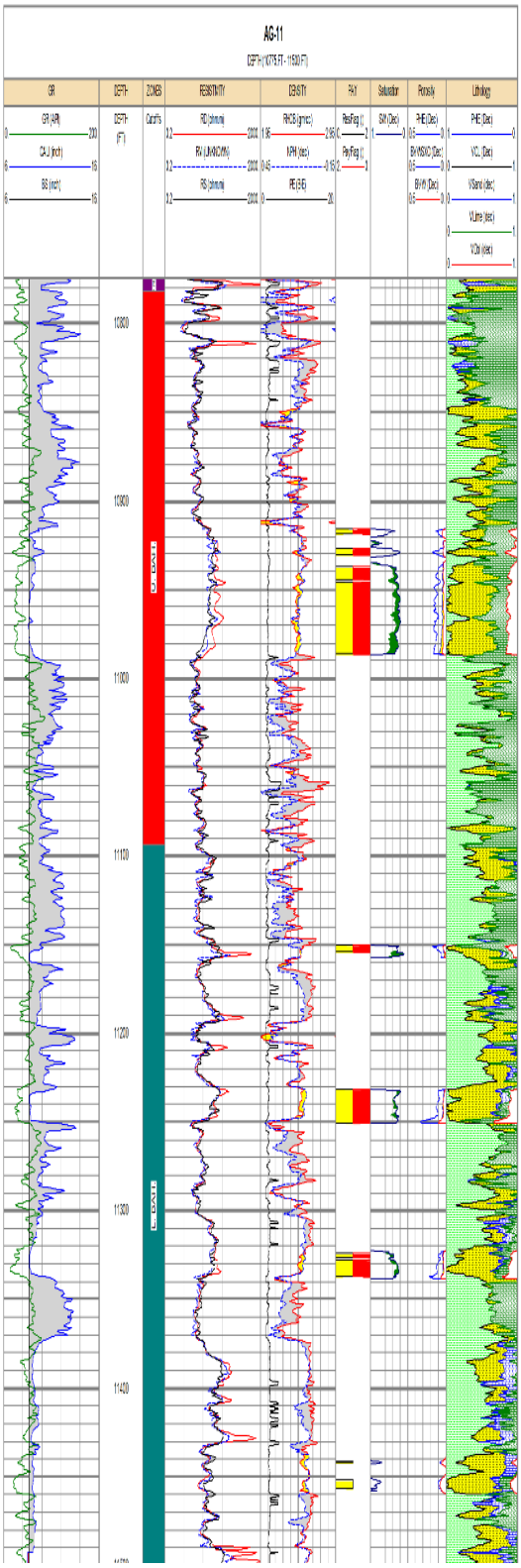

Fig. 15. Analog of Bahariya reservoirs (Upper & Lower) in AG-11 well.

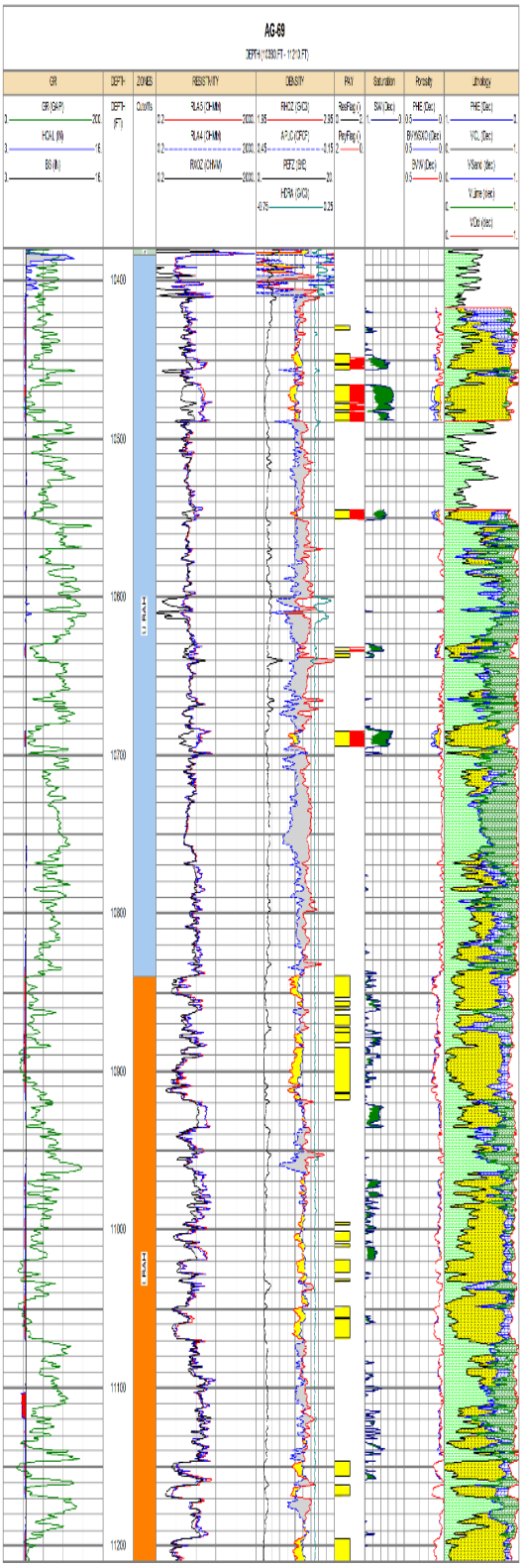

Fig. 16. Analog of Bahariya reservoirs (Upper & Lower) in AG-69 well.

To summarise, the Abu Roash (D & E) and (Upper & Lower) Bahariya rock units contain good reservoir zones, with varying lithologic compositions, that indicate various local depositional environments. Furthermore, both formations have high porosity, which supports oil and gas accumulation.

Acknowledgments

The authors are grateful to the Egyptian Petroleum Corporation (EGPC) and the Exploration Management of Khalda Petroleum Company (KPC) for supplying well data for this study, as well as the Schlumberger corporation for providing us with the Interactive Petrophysics software. We also thank Dr. **Mohamed Elbastawessy**, Assistant General Manager of the Petrophysics Department, and **Mr. Mohamed Elsawy**, Petrophysical Operation Department Head, both of them contributed to this study.

References

Asquith, G.B. and Gibson, C.R. (1982) Basic well log analysis for geologists. 1st edition, *AAPG Methods in Exploration Series, AAPG, Tulsa, Oklahoma, USA*, **3**, 216 p.

Helmy, B.M. (1990) Wrench faulting and its implication on hydrocarbon accumulations Alamein-Yidma area, Western Desert, Egypt. *Proceedings of 10th EGPC petroleum exploration and Production Conference*, **2**, 257-289.

Bigelow, L. (1995) Introduction to wireline log analysis. *Western Atlas International, Inc., Houston, Texas-USA*, 312 p.

EGPC (Egyptian General Petroleum Corporation) (1992) Western Desert, oil and Gas fields, a comprehensive overview. *11th EGPC Explor. and Prod. Conf, Cairo,*431 p.

Poupon, A. and Leveaux, J. (1971) Evaluation of water saturation in shaly parts of northern Egypt. *The Log Analyst*, **12**, 3-8.

Schlumberger (1972) The essential of log interpretation practice. *Schlumberger Ltd., France*, 45-67.

Schlumberger (1984) Geology of Egypt. *Well Evaluation Conference, Schlumberger, Cairo,* 1-64.

Schlumberger (1989) Principles Log Interpretation (Applications). *Schlumberger Educational Services*, 228 p.

Schlumberger (1995) Geology of Egypt. *Well Evaluation Conference, Schlumberger, Cairo,* 58-66.

Sultan, N. and Abd El-Halim, M.A. (1988) Tectonic framework of northern Western Desert, Egypt and its effect on hydrocarbon accumulations. *EGPC Ninth Exploration and production Conference, Cairo, Egypt.* **2**, 1-19.

Tearpock, D.J. and Bischke, R.E. (2003) Applied subsurface geological mapping. *Pearson Education, Inc. Publishing as Prentice Hall PTR, Upper Saddle River, New Jersey*, 822 p.

توصيف مكامن خزانات أبو رواش والبحرية لعصر الطباشيري العلوي، حقل نفط أبو الغراديق، شمال الصحراء الغربية، مصر

نادر حسني الجندي[١]، محمد عاطف نوير[١]، محمد صبحي الصادق[٢]، أحمد السيد علي[١]
[١]قسم الجيولوجيا، كلية العلوم، جامعة طنطا، طنطا ٣١٥٢٧، مصر
[٢]شركة خالدة للبترول، القاهرة، مصر

تقع منطقة الدراسة في حوض أبو الغراديق بين خطي عرض ‹٢٩ ° ٤٠ و ‹٢٩ ° ٤٥ شمالا وخطي طول ‹٢٨ ° ٢٥ و ‹٢٨ ° ٣٢ شرقا. تهدف هذه الدراسة إلى تقييم أربعة تكوينات صخرية تقع في المنطقة الوسطى في حوض أبو الغراديق، وتحديداً في حقل نفط أبو الغراديق، شمال الصحراء الغربية، مصر، من خلال إجراء التحليل البتروفيزيائي لدراسة الخزانات الحاملة للهيدروكربون لتكوينات العصر الطباشيري العلوي وهي أعضاء أبو رواش «D» و«E» بالإضافة إلى أعضاء تكوين البحرية.

من أجل تحقيق هذه الأهداف، تم استخدام برنامج البتروفيزيائية التفاعلية (IP)، الإصدار ٣,٥، لتقييم سجلات الآبار، وقدم البرنامج لنا العديد من العلاقات الثنائية المتقاطعة، وهي التوقيعات المتقاطعة لقيم تسجيلات النيوترونات والكثافة وتوقيعM-N، من أجل تحديد مسامية الخزانات وتكوينها وكذلك الإشارة إلى تأثير صخور الطفلة والمسامية الثانوية التي قد تؤثر على إمكانات جودة الهيدروكربون لهذه الخزانات. بالإضافة إلى ذلك، تم عمل علاقات للمحتويات الصخرية والسائلة لعدة تكوينات من منطقة الدراسة، تشير إلى التوزيع الرأسي للمعالم البتروفيزيائية لكل بئر في منطقة الدراسة، لإظهار توزيع حجم صخور الطفلة والمسامية وتشبع الماء والتشبع الهيدروكربوني. من بين أشياء أخرى، يكشف الأنالوج أيضًا عن وجود مناطق تحمل الزيت بدلالة عمق البئر.

ويؤكد تحليل البيانات البتروفيزيائية إلى أن خزان أبو رواش «D» يتكون في الغالب من الحجر الجيري مع الحجر الرملي، بالاضافة الي وجود طفلة، في حين أن خزان أبو رواش «E» يتكون أساسًا من الحجر الرملي، مع صخور الطفلة والحجر الجيري والدولوميت الصخري بينما الخزانات الموجودة في أعضاء تكوين البحرية العلوي والسفلى تتكون من صخور الحجرالرملي، مع بعض صخور الحجر الجيري والطفلة.

وتوصلت الدراسة إلى أن أحجام الصخر الزيتي في أبو رواش (D & E) والبحرية (العلوي والسفلي) هي ٠,٩ - ٣,٨٪، ٨,٢ - ١٣,٧، ٧,٢ - ١٥,٢، ٩ - ١٥,٥٪ على التوالي، والمسامية الفعالة هي ٦,٧ - ١٤,٧٪. ١٣,٩ - ١٨,١٪، ١٣,١ - ١٥,٥٪ و١١,٤ - ١٥,٥٪ مما يعبر عن جودة المكامن الصخرية الجيدة للمناطق. يتم عرض البيانات البتروفيزيائية من مكمن أبو رواش والبحرية على الأنالوج لتحديد الأماكن الأكثر فعالية داخل التكوينات الصخرية المختلفة وتحديد الأماكن الحاملة للهيدروكربونات الجيدة.